A correlation-based fuzzy cluster validity index with secondary options detector

Nathakhun Wiroonsri*and Onthada Preedasawakul [†]

Mathematics and Statistics with Applications Research Group (MaSA)
Department of Mathematics, King Mongkut's University of Technology Thonburi

Abstract

The optimal number of clusters is one of the main concerns when applying cluster analysis. Several cluster validity indexes have been introduced to address this problem. However, in some situations, there is more than one option that can be chosen as the final number of clusters. This aspect has been overlooked by most of the existing works in this area. In this study, we introduce a correlation-based fuzzy cluster validity index known as the Wiroonsri–Preedasawakul (WP) index. This index is defined based on the correlation between the actual distance between a pair of data points and the distance between adjusted centroids with respect to that pair. We evaluate and compare the performance of our index with several existing indexes, including Xie–Beni, Pakhira–Bandyopadhyay–Maulik, Tang, Wu–Li, generalized C, and Kwon2. We conduct this evaluation on four types of datasets: artificial datasets, real-world datasets, simulated datasets with second option, and image datasets, using the fuzzy c-means algorithm. Overall, the WP index outperforms most, if not all, of these indexes in terms of accurately detecting the optimal number of clusters and providing accurate secondary options. Moreover, our index remains effective even when the fuzziness parameter m is set to a large value. Our R package called UniversalCVI used in this work is available at `https://CRAN.R-project.org/package=UniversalCVI`.

Keyword: Cluster analysis, CRAN, fuzzy c-means (FCM), image processing, ranking, R package, sub-optimal.

1 Introduction

Cluster analysis is an unsupervised learning tool in machine learning that is widely used in various areas, including business, pattern recognition, data mining, medical diagnosis, and image processing, among others. It relies on the inherent properties, patterns, or similarities of objects to reveal meaningful information. The aim is to identify natural groupings within a dataset that are not initially apparent and without prior knowledge of the groups. There are several clustering algorithms, mainly categorized as centroid-based clustering (such as K-means, K-medoids, K-medians, and fuzzy c-means (FCM)), hierarchical clustering (including single linkage, complete linkage, group average agglomerative, and Ward's criterion), density-based clustering (such as DBSCAN, DENCLUE, and OPTICS), probabilistic clustering (EM), grid-based clustering (including CLIQUE, MAFIA, ENCLUS, and OptiGrid), and spectral clustering (for more details, refer to [1] and the references therein). More recently, deep learning clustering [2] and 3D point cloud techniques, such as PointNet, PointNet++, DGCNN, and RandLA-Net [3–5], have been introduced and have garnered significant

attention in this field. Recently, an alternative technique using random forest has also been introduced in [6]. A recent method based on both distance and density with the help of Apollonius function kernel is developed in [7].

In addition to the clustering process itself, there are two associated procedures: clustering tendency assessment and cluster validation. Clustering tendency assessment is a pivotal pre-clustering task that determines the presence of clusters in a dataset and, if detected, the optimal number of clusters to be sought. On the other hand, cluster validation involves evaluating the quality and performance of a clustering algorithm on a specific dataset (see [8]). A cluster validity index (CVI) serves as a tool capable of managing both of these procedures.

Cluster tendency is not necessary for certain algorithms like DBSCAN and OPTICS, where the number of clusters is determined automatically. However, it is essential for most clustering algorithms. In this study, our focus lies on centroid-based clustering, particularly the FCM algorithm. FCM, originally proposed by [9] and subsequently improved by [10], extends k-means by assigning a membership degree to each data point, indicating its likelihood of belonging to each group. Similar to k-means, determining the optimal number of clusters remains a prerequisite for FCM. Numerous studies have introduced and examined CVIs to ascertain the optimal number of clusters for FCM. Conventionally, the Partition Coefficient (PC) and Partition Entropy (PE), as defined in [11], rely solely on membership degrees. Most contemporary fuzzy CVIs are grounded in concepts of intercluster and intracluster distances, compactness, and separation. These include the Xie–Beni (XB) index [12], Fukuyama–Sugeno index [13], Pakhira–Bandyopadhyay–Maulik (PBM) index [14], Tang index [15], Wu–Li index (WL) [16], Kwon indexes (Kwon1 and Kwon2) [17,18], and Saraswat–Mittal (SMI) index [19]. A unique index, the generalized C (GC) index [20], incorporates the concept of Hubert's Gamma [21] to detect the strength of the relationship between the distance of each pair of data points and its membership degree. Alongside these categories, there exist a few approaches that utilize correlation to construct CVIs. For example, Pearson correlation and Spearman's (rho) correlation cluster validity [22] compute a correlation between pairwise distances and induced partition dissimilarity. During the process of preparing this manuscript, several works have developed new indices worth mentioning. The work [23] introduced a new fuzzy CVI intended for imbalanced datasets. In this study, we propose a novel correlation-based CVI as an additional option for users to choose from the extensive array of existing CVIs.

The primary objective of a CVI is unequivocally to determine the optimal number of clusters. However, certain scenarios might offer additional sub-optimal choices for selection. For example, in business, there can be multiple approaches to segment customers, or when dealing with cancer patients, multiple grouping strategies might apply. In image processing, a spectrum of optimal cluster numbers could effectively highlight the primary object within an image. This motivation drives the introduction of a novel index, termed the Wiroonsri–Preedasawakul (WP) index, designed to contribute to this field, particularly in the consistent provision of multiple optimal choices. The WP index finds its roots in the Wiroonsri index (WI), a hard CVI introduced in [24], which is exclusively compatible with k-means and hierarchical clustering. To be more precise, we propose a technique to transfer the key concept of the WI through new adjusted centroids compatible with any fuzzy clustering environment. The underlying concept is founded on a correlation between the actual distance separating a pair of data points and the distance between the adjusted centroids in relation to these points. One of the key benefits of using the original WI and the WP index is that they consistently produce multiple local optimums at different numbers of clusters. This feature allows users to choose the final number of clusters that best fits their specific applications. To the best of our knowledge, we are not aware of any works besides [24] discussed this point before.

While our index varies based on the dataset and is not directly employed for cluster validation, the essential correlation component can effectively fulfill this role. Given the myriad existing CVIs, we specifically compare our index to XB, PBM, Tang, WL, GC, and Kwon2. All the CVIs except

GC are selected as they are compatible with the same clustering algorithms, showcase exceptional performance, and are not tailored to specific dataset types. GC is selected since it is the most recent correlation-based fuzzy CVI we are aware of and hence it is worth to see the performance compared to ours. There are several more recent works published when we are preparing and revising our manuscript which are not in our comparison experiment. It is worth mentioning them here and we leave further analysis for future work. [25] uses an adjustment of within-cluster distance to define a new CVI. [26] defines a new CVI using topology structure instead of centroids. [27] proposes a hybrid CVI by weighted other known measures. [28] presents a new CVI using the fuzzy set theory. [29–32] introduce new CVIs intended for some specific situations such as data with missing values, and hyperellipsoid or hyperspherical data.

The rest of this work is organized as follows. Section 2 provides essential background information regarding FCM and existing CVIs. Our proposed index, along with its mathematical properties and complexity, are presented in Section 3. Experimental results, including those from image processing, are detailed in Section 4. The concluding remarks and potential future directions are discussed in Section 5.

2   Background

In this section, we revisit the FCM algorithm and introduce six established fuzzy CVIs with which we will compare the performance of our proposed index. Let $n, c \in \mathbb{N}$, subject to the condition $c \leq n$, $i \in [n]$, and $j \in [c]$, where for $k \in \mathbb{N}$, we denote $[k] = \{1, 2, \ldots, k\}$. The subsequent notations will be utilized throughout the remainder of this work.

1. x_i: Data points

2. c: Number of clusters

3. C: Known actual number of clusters

4. C_j: Set of data points in the jth cluster

5. v_j: j^{th} cluster centroid

6. v_0: Centroid of the entire data

7. $\bar{v}$: Centroid of all v_j

8. $\mu = (\mu_{ij})$: Membership degree matrix where μ_{ij} denotes the degree to which a sample point x_i belongs to C_j.

9. $\|x - y\|$: Euclidean distance between x and y.

2.1   Fuzzy c-means

FCM clustering is a soft centroid-based clustering technique introduced by [9], and later refined by [10]. This method involves iteratively updating c centroids and the membership degree that assigns each point to each cluster, ranging from 0 to 1, until convergence is achieved or a predetermined maximum number of iterations is reached. The objective of FCM is to minimize a specific function,

$$\sum_{i=1}^{n} \sum_{j=1}^{c} \mu_{ij}^m \|x_i - v_j\|^2, \tag{1}$$

where $m > 1$ denotes the fuzziness parameter.

Initially, by randomizing centroids v_j, the optimization of (1) is performed through the iterative update of membership degrees,

$$\mu_{ij} = \frac{1}{\sum_{k=1}^{c} \left(\frac{\|x_i - v_j\|}{\|x_i - v_k\|} \right)^{\frac{2}{m-1}}}, \tag{2}$$

and the centroids,

$$v_j = \frac{\sum_{i=1}^{n} \mu_{ij}^m x_i}{\sum_{i=1}^{n} \mu_{ij}^m}, \tag{3}$$

for $i, j \in \{1, 2, \ldots, n\}$.

2.2   Existing fuzzy cluster validity indexes

In this study, we assess the performance of our newly introduced index in comparison to six existing indices, which are defined as follows.

Xie–Beni index [12]

The XB index evaluates the compactness and separation of fuzzy c-partitions. It relies on various factors such as distances between data points and centroids, membership degree, and the minimum distance between centroids. The XB index is defined as

$$\mathrm{XB(c)} = \frac{\sum_{j=1}^{c} \sum_{i=1}^{n} \mu_{ij}^2 \|x_i - v_j\|^2}{n \cdot \min_{j \neq k} \{\|v_j - v_k\|^2\}}.$$

The lowest value of XB(c) indicates a valid optimal partition.

Pakhira–Bandyopadhyay–Maulik index [14]

The PBM index is defined similarly to XB, with the main difference lying in the exponent of the main term and the replacement of the minimum with the maximum. The PBM index is defined as

$$\mathrm{PBM(c)} = \left(\frac{\sum_{i=1}^{n} \|x_i - v_0\| \cdot \max_{j \neq k} \|v_j - v_k\|}{c \sum_{j=1}^{c} \sum_{i=1}^{n} \mu_{ij} \|x_i - v_j\|} \right)^2.$$

The largest value of PBM(c) indicates a valid optimal partition.

Tang index [15]

The Tang index is derived from the XB index by incorporating the sum of distances between cluster centroids in the numerator. This addition addresses issues related to the monotonically decreasing trend and numerical instability. The Tang index is defined as

Tang(c)

$$= \frac{\sum_{j=1}^{c} \sum_{i=1}^{n} \mu_{ij}^2 \|x_i - v_j\|^2 + \frac{1}{c(c-1)} \sum_{j \neq k} \|v_j - v_k\|^2}{\min_{j \neq k} \{\|v_j - v_k\|^2\} + \frac{1}{c}}.$$

The smallest value of Tang(c) indicates a valid optimal partition.

Wu–Li index [16]

The WL index evaluates the overall compactness-separation ratio of all clusters and each individual cluster. By introducing a median factor, it addresses instability issues arising in other CVIs under the same root when two centroids are closely allocated. The Wu–Li index is defined as

$$\text{WL(c)} = \frac{\sum_{j=1}^{c} \left(\dfrac{\sum_{i=1}^{n} \mu_{ij}^2 \|x_i - v_j\|^2}{\sum_{i=1}^{n} \mu_{ij}} \right)}{\min_{j \neq k}\{\|v_j - v_k\|^2\} + \text{median}_{j \neq k}\{\|v_j - v_k\|^2\}}.$$

The smallest value of WL(c) indicates a valid optimal partition.

Generalized C index [20]

The GC index is a soft version of the C-index, formulated based on relational transformations of the membership degree matrix μ. It comprises four distinct variants, each with its own definition. Let

$$R_\otimes(\mu) = \mu \otimes \mu^T$$

where $\otimes$ represents one of the following matrix products: $\sim$ Sum–Product, $\sim$ Sum–Min, $\sim$ Max–Product, and $\sim$ Max–Min. Denoting $R_\otimes(\mu) = [r_{ij}(\mu)]$, the Generalized Hubert's Gamma is defined as

$$\Gamma_\otimes = \sum_{j=i+1}^{n} \sum_{i=1}^{n-1} r_{ij}(\mu) \cdot \|x_i - x_j\|. \tag{4}$$

Moreover, let

$$n_{\text{ws}} = \left\lfloor \frac{\sum_{j=1}^{c} \left(\sum_{i=1}^{n} \mu_{ij} \right) \left(\sum_{i=1}^{n} \mu_{ij} - 1 \right)}{2} \right\rfloor.$$

The GC index is then defined as

$$\text{GC(c)} = \frac{\Gamma_\otimes - min(\Gamma_\otimes)}{max(\Gamma_\otimes) - min(\Gamma_\otimes)},$$

where $max(\Gamma)$ is computed similarly to (4), but the sum is taken over the first n_{ws} terms after rearranging $|x_i \check{\ } x_j|$ and $r_{ij}(\mu)$ in descending order, and $min(\Gamma_\otimes)$ is computed similarly to $max(\Gamma_\otimes)$, but with $r_{ij}(\mu)$ arranged in ascending order. Notably, in this study, we consider only the $(\sum \wedge)$ version, as it delivers the best results in our experiments. The smallest value of GC(c) indicates a valid optimal partition.

Kwon2 index [18]

The Kwon2 index is a generalization of the Kwon index and is designed to address three main challenges present in the original Kwon index: issues that arise when the number of clusters approaches the number of data points, numerical instability with larger fuzziness parameter (m), and underestimation of the true number of clusters. The Kwon2 index is defined as

Kwon2(c)

$$= \frac{w_1 \left[w_2 \sum_{j=1}^{c} \sum_{i=1}^{n} \mu_{ij}^{2\sqrt{\frac{m}{2}}} \|x_i - v_j\|^2 + \dfrac{\sum_{j=1}^{c} \|v_j - v_0\|^2}{\max_j \|v_j - v_0\|^2} + w_3 \right]}{\min_{i \neq j} \|v_i - v_j\|^2 + \frac{1}{c} + \frac{1}{c^{m-1}}}$$

where $w_1 = \frac{n-c+1}{n}$, $w_2 = \left(\frac{c}{c-1}\right)^{\sqrt{2}}$ and $w_3 = \frac{nc}{(n-c+1)^2}$. The smallest value of Kwon2(c) indicates a valid optimal partition.

3 Our proposed index

In this section, we present the definition of our proposed index, establish some mathematical properties, and delve into its computational complexity.

3.1 Definition

Our newly introduced index draws inspiration from the recently developed Wiroonsri index [24], tailored for hard clustering methods exclusively. In the fuzzy context, however, there's a distinction: rather than having precise knowledge of the cluster centroid occupied by each sample point, we possess only the membership degree indicating the likelihood of the sample point belonging to each cluster. This necessitates the introduction of an adjusted centroid in relation to each sample point. Adopting the same notations as defined in Section 2, let

$$o_i(c, \gamma) = \frac{\sum_{j=1}^c \mu_{ij}^\gamma v_j}{\sum_{j=1}^c \mu_{ij}^\gamma} \tag{5}$$

be an adjusted centroid corresponding to the membership degree of x_i, and let $\gamma > 0$ signify an adapted fuzziness parameter for our index. Additionally, let

$$\vec{d}_v = (\|x_i - v_0\|)_{i \in [n]} \tag{6}$$

be a vector of length n encompassing the distances of all data points to the centroid of the entire dataset. Further, let

$$\vec{d} = (\|x_i - x_j\|)_{i,j \in [n]} \tag{7}$$

be a vector of length $\binom{n}{2}$ containing distances between all pairs of data points, and

$$\vec{v}(c) = (\|o_i(c, \gamma) - o_j(c, \gamma)\|)_{i,j \in [n]} \tag{8}$$

be another vector of the same length, denoting the distances between pairs of respective adjusted centroids associated with the membership degrees of the two points. It is important to note that, throughout this work, we exclusively employ the Euclidean distance. We proceed by introducing the ensuing correlation, built upon the aforementioned adjusted centroid concept.

Definition 3.1 *Let $\vec{d}$ and $\vec{v}(c)$ be as in 7 and 8, respectively. WP correlation is defined as*

$$WPC(c) = \mathrm{Corr}(\vec{d}, \vec{v}(c))$$

for $c = 2, 3, \ldots, n$, and

$$WPC(1) = 0 \quad or \quad WPC(1) = \frac{SD(\vec{d}_v)}{\max \vec{d}_v - \min \vec{d}_v}$$

where $\mathrm{Corr}(\cdot, \cdot)$ denotes a correlation coefficient.

In this work, we only consider Pearson correlation which is defined as

$$\mathrm{WPC}(c) = \frac{\sum_{i,j \in [n]} (d_{ij} - \bar{d})((v_{ij}(c) - \bar{v}(c)))}{\sqrt{\sum_{i,j \in [n]} (d_{ij} - \bar{d})^2} \sqrt{\sum_{i,j \in [n]} (v_{ij}(c) - \bar{v}(c))^2}}.$$

The user must select one of the two options for WPC(1). If WPC(1) = 0 is chosen, then WPC(2) often exhibits significant improvement compared to WPC(1), frequently resulting in an optimal number of clusters at $c = 2$. On the other hand, when WPC(1) is determined by the ratio of the standard deviation (SD) and the discrepancy between the maximum and minimum distances of each data point from the centroid of the entire dataset, it can lead to improved outcomes. The rationale is intuitive: when the SD is substantially smaller than the difference between the maximum and minimum distances, dividing the dataset into two groups can yield a more effective partition. A substantial WPC value (close to 1) signifies a strong linear relationship between the actual distance and the distance of corresponding adjusted centroids based on the membership degrees of the two points. Subsequent subsections will reveal that WPC(c) becomes significant as c approaches n, with WPC(n) = 1. However, clustering n observations into n groups is not the purpose of performing cluster analysis. According to discussions in [24], WPI1 and WPI2 quantify the enhancements in WPC when the number of clusters is increased or decreased by one. For $c = 2, 3, \ldots, n - 1$, let

$$
\begin{aligned}
\text{WPI1}(c) &= \frac{\text{WPC}(c) - \text{WPC}(c - 1)}{1 - \text{WPC}(c - 1)} \Bigg/ \frac{\max\{0, \text{WPC}(c + 1) - \text{WPC}(c)\}}{1 - \text{WPC}(c)} \\
&= \frac{(\text{WPC}(c) - \text{WPC}(c - 1))\,(1 - \text{WPC}(c))}{\max\{0, \text{WPC}(c + 1) - \text{WPC}(c)\}\,(1 - \text{WPC}(c - 1))}
\end{aligned}
\tag{9}
$$

and

$$
\text{WPI2}(c) = \frac{\text{WPC}(c) - \text{WPC}(c - 1)}{1 - \text{WPC}(c - 1)} - \frac{\text{WPC}(c + 1) - \text{WPC}(c)}{1 - \text{WPC}(c)}.
\tag{10}
$$

With all the necessary components introduced, our proposed index is defined as follows.

Definition 3.2 *Let $p \in [n - 1]\backslash\{1\}$, WPC be as in Definition 3.1 and WPI1 and WPI2 be as in* (9) *and* (10), *respectively. For $c = 2, 3, \ldots, p$, WP index is defined as*

Case 1: $\max_{2 \leq l \leq p} \text{WPI1}(c) < +\infty$ *and* $\exists l \in [p]\backslash\{1\}$ *such that* $|\text{WPI1}(l)| < \infty$.

$$
WP_p(c) = \begin{cases} \min_{2 \leq l \leq p}\{\text{WPI1}(l)\,|\,\text{WPI1}(l) > -\infty\} & \text{if } \text{WPI1}(c) = -\infty \\ \text{WPI1}(c) & \text{otherwise.} \end{cases}
$$

Case 2: $\max_{2 \leq l \leq p} \text{WPI1}(c) = +\infty$ *and* $\exists l \in \{2, 3, \ldots, p\}$ *such that* $|\text{WPI1}(l)| < \infty$.

$$
WP_p(c) = \begin{cases} \min_{2 \leq l \leq p}\{\text{WPI1}(l)\,|\,\text{WPI1}(l) > -\infty\} + \text{WPI2}(c) & \text{if } \text{WPI1}(c) = -\infty \\ \max_{2 \leq l \leq p}\{\text{WPI1}(l)\,|\,\text{WPI1}(l) < +\infty\} + \text{WPI2}(c) & \text{if } \text{WPI1}(c) = +\infty \\ \text{WPI1}(c) + \text{WPI2}(c) & \text{otherwise.} \end{cases}
$$

Case 3: $\forall l \in \{2, 3, \ldots, p\}$, $|\text{WPI1}(l)| = +\infty$.

$$
WP_p(c) = \text{WPI2}(c).
$$

Clearly, the largest value of $\text{WP}_p(c)$ indicates a valid optimal partition. Since our index is slightly more intricate compared to most existing ones, we provide an algorithm for computing the WP index for FCM with $c = 2, 3, \ldots, p$ in Algorithm 1. The fuzziness parameter for our index, denoted as $\gamma > 0$, is set by default to $7m^2/4$, where m is the fuzziness parameter of FCM. However, this value can be adjusted by the user. A remark below clarifies the significance of γ and our choice of a moderate default value, which enhances the stability of our index while still maintaining a connection to the fuzziness level of the clustering method. It's important to note that FCM can be substituted with any other clustering method that employs a membership degree matrix.

Algorithm 1 WP index for FCM

Input: x, $cmin$, $cmax$, m, γ (default= $7m^2/4$)
Output: WP index where $p = cmax$ for FCM with c from $cmin$ to $cmax$
    1. Compute the vector of distances between all pairs of data points $\vec{d}$;
    2. Set up the lower and upper bounds to compute WPC;

        if $cmin = 2$, **then** $lb = 2$;

        else $lb = cmin - 1$

    3. Compute WPC(c) correlation;

        For c from lb to $cmax + 1$;

            3.1 Cluster x using FCM with fuzziness m

            3.2 Compute adjusted centroids as in (5)

            3.3 Compute WPC as in Definition 3.1

        End For

    4. Compute $\texttt{WPI1}(c)$ and $\texttt{WPI2}(c)$ for c from $cmin$ to $cmax$
    5. Compute $\texttt{WP}_p(c)$ where $p = cmax$ for c from $cmin$ to $cmax$

        if $\forall c, |\texttt{WPI1}(c)| = \infty$, **then** $\texttt{WP}_p(c) = \texttt{WPI2}(c)$;

        else if $\forall c, \texttt{WPI1}(c) < \infty$,

        then $\texttt{WP}_p(c) = \max\{\texttt{WPI1}(c), \min_l\{\texttt{WPI1}(l) > -\infty\}\}$;

        else $\texttt{WP}_p(c) = \texttt{WPI2}(c) + \min\big\{\max_l\{\texttt{WPI1}(l) < \infty\}, \max\{\texttt{WPI1}(c), \min_l\{\texttt{WPI1}(l) > -\infty\}\}\big\}$

    Return $\texttt{WP}_p(c)$ where $p = cmax$ for c from $cmin$ to $cmax$

Remark 3.3 *We discuss the following situations to illustrate the three cases in Definition 3.2 of the WP index. For simplicity, we consider* **cmin**= 2 *and* **cmax**= 4*.*

    Case 1: *Assume that* $\texttt{WPC} = (0.4, 0.7, 0.9, 0.95, 0.97)$*. Then* $\texttt{WPI1} = (0.75, 1.33, 1.25)$*. This falls into Case 1 and thus* $\texttt{WP} = \texttt{WPI1} = (0.75, 1.33, 1.25)$

    Case 2: *Assume that* $\texttt{WPC} = (0.4, 0.7, 0.9, 0.85, 0.92)$*. Then* $\texttt{WPI1} = (0.75, +\infty, -1.07)$ *and* $\texttt{WPC2} = (-0.17, 1.17, -0.97)$*. This falls into Case 2 and thus* $\texttt{WP} = (0.75 - 0.17, 0.75 + 1.17, -1.07 - 0.97) = (0.58, 1.92, -2.04)$

    Case 3: *Assume that* $\texttt{WPC} = (0.4, 0.9, 0.8, 0.7, 0.6)$*. Then* $\texttt{WPI1} = (+\infty, -\infty, -\infty)$ *and* $\texttt{WPI2} = (1.83, -0.5, -0.17)$*. This falls into Case 3 and thus* $\texttt{WP} = \texttt{WPI2} = (1.83, -0.5, -0.17)$

Remark 3.4 *The range of the WP index is dataset-dependent and therefore cannot be directly employed for evaluating the quality of clustering outcomes. However, the auxiliary metric WPC, necessary for calculating the WP index, can be employed for this assessment. It's worth noting that a WPC value approaching one signifies favorable clustering performance.*

3.2 Some properties related to the WP index

In this subsection, we present and substantiate several properties associated with the WPC and the concept of adjusted centroids. We initiate with the following lemma, which addresses the computation of centroids and membership degrees in FCM for the specific scenario when $c = n$.

Lemma 3.5 *For $n \in \mathbb{N}$ and $i \neq j \in [n]$, let v_i and μ_{ij} be the centroid and the membership degree from the FCM algorithm with $c = n$. Then*

1. $v_i = x_i$,

2. $\mu_{ii} = 1$ and $\mu_{ij} = 0$.

Proof:

Since c is set to be n, for any $\epsilon > 0$, we can let $x_i^* = (x_{i1} + \epsilon, x_{i2}, \ldots, x_{ip})$ be the initial centroids. Then, by (2),

$$\mu_{ii} = \frac{1}{\sum_{k=1}^{c} \left(\frac{\|x_i - x_i^*\|}{\|x_i - x_k^*\|} \right)^{\frac{2}{m-1}}} = \frac{1}{1 + \sum_{k \neq i} \left(\frac{\epsilon}{c_{k,\epsilon}} \right)^{\frac{2}{m-1}}}$$

where $c_{k,\epsilon} = \|x_i - x_k^*\|$. As ϵ is arbitrary, by taking $\epsilon \to 0$, we have $c_{k,\epsilon} \to \|x_i - x_k\|$ for $k \neq i$, and hence $\mu_{ii} = 1$. It follows that $\mu_{ij} = 0$ for $j \neq i$. Clearly, if we further update the centroids as in (3), then they remain the same. $\qquad\square$

Next we prove the following properties of the adjusted centroids.

Proposition 3.6 *Let $n, c \in \mathbb{N}$ such that $c \leq n$, and $o_i(c, \gamma)$ be as in (5). Then the followings hold.*

1. *For any $i \in [n]$, if $\mu_{ij} \neq 0$ for all $j \in [c]$, then $\lim_{\gamma \downarrow 0} o_i(c, \gamma) = \frac{1}{c} \sum_{j=1}^{c} v_j = \bar{v}$.*

2. *For $i \in [n]$, if $\mu_{ij} \neq \mu_{ik}$ for all $j \neq k$, then there exists $j \in [c]$ such that $\lim_{\gamma \uparrow \infty} o_i(c, \gamma) = v_j$.*

3. *If $c = n$, $o_i(c, \gamma) = x_i$ for all $i \in [n]$ and $\gamma > 0$.*

Proof:

1) Since $\mu_{ij} \neq 0$ for all j,

$$\lim_{\gamma \downarrow 0} o_i(c, \gamma) = \lim_{\gamma \downarrow 0} \left(\frac{\sum_{j=1}^{c} \mu_{ij}^{\gamma} v_j}{\sum_{j=1}^{c} \mu_{ij}^{\gamma}} \right) = \frac{\sum_{j=1}^{c} \mu_{ij}^{0} v_j}{\sum_{j=1}^{c} \mu_{ij}^{0}}$$

$$= \frac{1}{c} \sum_{j=1}^{c} v_j = \bar{v}.$$

2) Since $\mu_{ij} \neq \mu_{ik}$ for all $j \neq k$, we can without loss of generality assume that $\max_k \mu_{ik} = \mu_{ij}$. Dividing the top and the bottom of $o_i(c, \gamma)$ by μ_{ij}^{γ}, we have

$$\lim_{\gamma \uparrow \infty} o_i(c, \gamma) = \lim_{\gamma \uparrow \infty} \left(\frac{\sum_{k=1}^{c} \mu_{ik}^{\gamma} v_k}{\sum_{k=1}^{c} \mu_{ik}^{\gamma}} \right)$$

$$= \lim_{\gamma \uparrow \infty} \left(\frac{v_j + \left(\sum_{k \neq j} \left(\frac{\mu_{ik}}{\mu_{ij}} \right)^{\gamma} v_k \right)}{1 + \sum_{k \neq j} \left(\frac{\mu_{ik}}{\mu_{ij}} \right)^{\gamma}} \right) = v_j.$$

3) By Lemma 3.5, it is clear that

$$o_i(c, \gamma) = \frac{\sum_{j=1}^{n} \mu_{ij}^{\gamma} x_j}{\sum_{j=1}^{n} \mu_{ij}^{\gamma}} = x_i.$$

$\qquad\square$

Next we discuss some properties of the adjusted centroid in the following Remark.

Remark 3.7   *1. A larger γ results in the calculation of $o_i(c, \gamma)$ with more emphasis on the largest membership degree cluster corresponding to that data point. This, in turn, leads to greater stability of the index.*

2. When γ approaches zero, the values of $o_i(c, \gamma)$ for each data point tend to converge to the same point. Consequently, the overall stability of our index diminishes under these conditions.

3. The special case where $\gamma = 1$ implies that $o_i(c, \gamma)$ is determined based solely on the original membership degree of the data point.

We end this subsection by stating the properties of WPC.

Proposition 3.8 *For $c \in [n]$ and $WPC(c)$ as in Definition 3.1,*

1. $-1 \leq WPC(c) \leq 1$

2. $WPC(n) = 1$ *when applying FCM with sufficient number of iterations.*

Proof:

The first item follows immediately from the fact that Corr is a correlation coefficient and that $|WPC(1)| \leq 1$.

To prove the second item, it follows from Lemma 3.5 that $\vec{v}(n) = \vec{d}$. Therefore, $WPC(n) = Corr(\vec{d}, \vec{d}) = 1$. $\qquad\qquad\square$

3.3 Complexity analysis

Table 1: CVIs complexities

Index	Complexity
XB, PBM, TANG, WL, and KWON2	$O(cp(c + n)$
GC	$O((c + p + \log n)n^2)$
WP	$O(p(c^2 + n^2))$

Table 1 displays the big O complexity of each index examined in this study. It is evident that our index is more complex by $O(n)$ compared to most of the existing indexes, except for GC. While WP is $O(\log n)$ faster than GC, both GC and our proposed index prove unsuitable for large-scale data. The high complexity of the WP index results from the fact that it requires computing the distances between all $\binom{n}{2}$ pairs of data points. However, the subsequent section outlines how WP can be effectively applied to image processing, a field characterized by extensive data. Notably, WP not only surpasses existing indexes in accuracy but also offers certain advantages that justify its utilization.

4 Experimental results

In this section, we perform two main experiments in the following two subsections. The first devotes to the sensitivity analysis of our index on its parameter γ and the latter includes applications of our proposed index on four different types of datasets compared to others. To facilitate our experiment, we employ our dedicated R package called "UniversalCVI" ([33]) through the RStudio environment ([34]). The "cmeans" function from the "e1071" package ([35]) is also employed for the computation of all the listed indexes.

Figure 1: Small datasets for sensitivity analysis
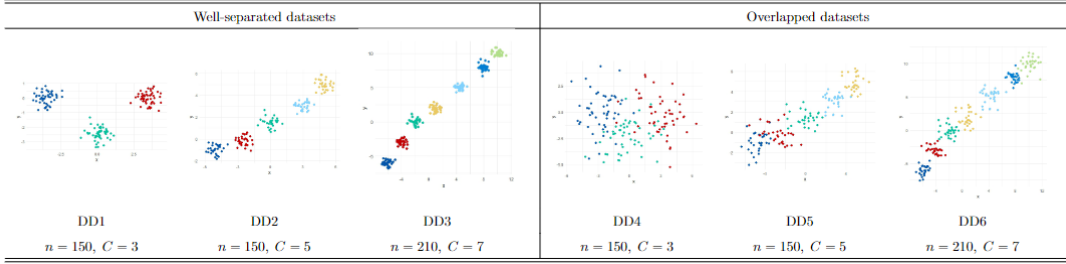
Note: n and C are the number of data points and the true number of clusters, respectively.

4.1 Sensitivity analysis on fuzziness parameter

In this subsection, we analyze the sensitivity of the WP index according to the fuzziness parameter γ defined in (5) and discuss how the default parameter is set based on some additional experiments.

By Proposition 3.6, when γ is very small, each adjusted centroid is close to the centroid of the entire dataset. This causes all the adjusted centroids to be sensitive and close to each other which results in extremely unstable WPC and thus the WP index. On the other hand, when γ is large, each adjusted centroid converges to one of the c centroids from the FCM. This may lead to slightly high sensitivity as well in some situations, however, by this condition, it should be fitted well with well-separated datasets. Therefore, when datasets are blind, we set a moderate default parameter as $7m^2/4$ where m is the fuzziness parameter of FCM. Note that we came up with this specific value by too detailed and lengthy experiment which is omitted from the paper.

Table 2: Standard deviations of the WP index from 100 times according to γ

| Data | C | γ | c | | | | | | | | | Average |
			2	3	4	5	6	7	8	9	10	
		1	0.10	18.41	0.76	0.78	29.19	3.76	4.02	22.87	7.97	9.76
DD1	3	7	0.05	2.89	0.73	0.46	0.90	0.61	0.68	1.32	6.44	1.57
		100	0.06	3.99	0.79	0.50	0.82	0.72	0.54	0.88	1.93	**1.14**
		1	0.20	0.13	0.24	79.91	29.26	20.32	80.33	24.29	78.04	34.75
DD2	5	7	0.12	0.27	0.23	3.87	1.10	1.76	2.57	3.41	4.41	1.97
		100	0.08	0.68	0.23	4.68	1.15	1.36	1.98	2.79	4.71	**1.96**
		1	0.06	0.14	0.25	0.81	0.56	364.84	11.26	9.87	133.21	57.89
DD3	7	7	0.10	0.17	0.14	0.17	0.19	13.33	1.66	11.73	10.85	4.26
		100	0.08	0.06	0.24	0.21	0.15	15.60	1.93	7.89	11.25	**4.16**
		1	1.00	7.73	27.77	4.90	7.70	32.71	9.88	20.22	28.77	15.63
DD4	3	7	0.31	1.53	0.50	0.65	0.83	0.85	1.34	0.93	10.32	**1.92**
		100	0.32	1.53	0.57	1.16	0.91	0.79	12.63	1.43	2.28	2.40
		1	0.24	0.62	0.46	37.44	299.25	36.47	298.99	8.69	20.77	78.10
DD5	5	7	0.09	0.94	0.17	17.68	1.41	1.36	3.15	1.65	6.45	**3.66**
		100	0.07	1.30	0.18	31.20	1.44	2.08	9.49	2.45	3.07	5.70
		1	0.04	0.16	0.51	0.81	1.39	9.89	39.66	11.96	38.93	11.48
DD6	7	7	0.09	0.13	0.16	0.11	0.15	8.09	5.28	5.41	7.33	**2.97**
		100	0.10	0.09	0.23	0.19	0.20	13.91	2.48	6.35	3.77	3.04

Note: the smallest average standard deviations are in bold.

To illustrate the situation, we generate six small datasets from Gaussian distributions for 100 times each as shown in Figure 1. The first three datasets are well-separated while the latter three are overlapped. Then we compute the WP index for $\gamma \in \{1, 7, 100\}$ based on the FCM algorithm with $m = 2$. Table 2 reports the standard deviations (SD) of $\mathrm{WP}(c)$ for c from 2 to 10 and their average from 100 generated datasets from the same distributions. As expected, the average SD for $\gamma = 100$ and $\gamma = 7$ are the smallest in the well-separated and the overlapped cases, respectively. Though the large γ provides the least sensitivity in the well-separated case, the moderate one gives acceptably low sensitivity in both cases. Obviously, the small γ provides extremely high sensitivity in all cases.

Table 3: Sensitivity of the WP index results from 10 rounds

Well-seperated datasets							Overlapped datasets						
			Rank							Rank			
Data	C	γ	1	2	3	4	Data	C	γ	1	2	3	4
DD1	3	1	1^{10}				DD4	3	1	3^3	4^7		
		7	1^{10}						7	1^7	2^3		
		100	1^{10}						100	1^7	2^3		
DD2	5	1	1^3	2^2	3^4	4^1	DD5	5	1	5^7	6^3		
		7	1^9	2^1					7	1^5	2^3	3^1	4^1
		100	1^{10}						100	1^4	2^5	3^1	
DD3	7	1	1^{10}				DD6	7	1	1^6	2^4		
		7	1^{10}						7	1^9	2^1		
		100	1^{10}						100	1^4	2^6		

Note: the numbers shown in the table are the rank for which the actual number of clusters corresponds and the subscripts are the number of times from 10 times.

Furthermore, we perform another experiment on the six datasets generated only once from the previous distributions. The WP index is computed for 10 times on each dataset based on the FCM algorithm with $m = 2$. In Table 3, we record the rank for which the actual number of clusters corresponds and the number of times it falls into that rank in the superscript. Obviously, the moderate γ provides the best results overall and low sensitivity, though the larger γ performs slightly better on well-separated datasets. Again, the small γ gives the worst result.

As users do not usually know whether their datasets are well-separated or not, our default parameter is recommended and will be used in the remaining of the work.

4.2 Applications to four types of datasets

In this subsection, we demonstrate the efficacy of our proposed index by conducting a comprehensive experiment. Our experiment is divided into four distinct parts, each detailed in separate subsections: artificial datasets (D1–D20), real-world datasets, simulated datasets with second option (R1–R7), and image datasets (IMG1–IMG5). For our analysis, we utilize the FCM algorithm on all normalized datasets. We set the fuzziness factor to $m = 1.5, 2, 4$ for the first two parts, which is well within the compatible range for most cases (as outlined in [36]). For the datasets with second option and image datasets, we only set $m = 2$ since our main focus is to evaluate the secondary option detection performance.

Since all the datasets we consider are labeled, Table 4 assesses the compatibility of the main clustering algorithm, FCM, with different values of m on these datasets. Specifically, we compute the proportion of data points correctly assigned to their respective groups when setting the number of clusters, c, to match the actual number of groups in the dataset. We utilize our WPfuzzyCVIs

package for this algorithm. It's essential to note that if FCM demonstrates sub-optimal performance on any dataset, showcasing the efficiency of indexes based on it becomes redundant. Consequently, for a given value of m, we avoid considering artificial datasets with an accuracy of less than 75%, and real-world datasets with an accuracy of less than 70% when selecting the correct value of c. An overview of the results is provided in Table 4.

Table 4: The proportion of sample points assigned into the true groups by c-means with $m = 1.5, 2, 4$

Dataset	m		
	1.5	2	4
Artificial datasets			
D1	1.000	1.000	1.000
D2	1.000	1.000	1.000
D3	1.000	1.000	1.000
D4	1.000	1.000	1.000
D5	0.997	0.997	0.743*
D6	0.926	0.926	0.924
D7	0.980	0.979	0.980
D8	0.986	0.986	0.987
D9	0.954	0.954	0.952
D10	0.985	0.978	0.969
D11	1.000	1.000	0.726*
D12	0.955	0.954	0.961
D13	0.914	0.913	0.911
D14	0.940	0.939	0.932
D15	0.915	0.914	0.914
D16	0.953	0.953	0.953
D17	1.000	1.000	0.993
D18	1.000	0.999	0.999
D19	0.975	0.963	0.952
D20	0.993	0.991	0.993
Real world datasets			
BCW	0.916	0.914	0.916
SEED	0.924	0.919	0.900
ION	0.701	0.701	0.701
Iris 2	1.000	1.000	0.993
Iris 3	0.833	0.840	0.853
Wine	0.966	0.966	0.567
Simulated datasets with ranks			
R1	-	1.000	-
R2	-	0.999	-
R3	-	1.000	-
R4	-	1.000	-
R5	-	0.992	-
R6	-	0.941	-
R7	-	0.973	-

Note: The proportions less than 0.75 for artificial and 0.7 for real-world datasets are marked with *

Given FCM's susceptibility to initial randomization, which in turn affects the sensitivity of validity indexes, we undertake a robust approach for our experiment. We execute FCM for a total of 20 rounds and select the round where the objective function in (1) yields the smallest value. This

approach ensures that the indexes' performance is evaluated under conditions of minimal objective function values. Alternatively, an approach suggested in [19] involves computing indexes across all rounds of FCM and selecting the most frequently occurring optimal c. However, we maintain our stance that if the primary clustering method yields sub-optimal results in a given round, it's not pragmatic to compute indexes based on those results.

For comparing the efficacy of all indexes, we apply FCM to each normalized dataset, varying the number of clusters from two to $c_{\max}$, where

$$cmax = \begin{cases} 10 & \text{if } 2 \leq C \leq 8 \\ 15 & \text{if } 9 \leq C \leq 13 \\ 20 & \text{if } 14 \leq C \leq 18. \end{cases}$$

Given that [20] presents four alternative indexes, we specifically report on the second alternative, $C(\Sigma\wedge)$, which consistently yields the best outcomes in our experiments. Additionally, it's important to note that the fuzziness parameter γ for our index is set to the default value of $7m^2/4$ in all experiments conducted.

4.2.1 Artificial datasets

In this subsection, we focus on artificial datasets, which we classify into distinct groups based on their characteristics. These datasets include both benchmark datasets (D3, D4, D8) from [37], as well as those we simulated ourselves (D1, D2, D9–D14, D19, D20) available in [38], with additional datasets sourced from [39] (D5–D7, D15–D18). The datasets are categorized into the following groups.

Group1: well-separated $D1 - D4$
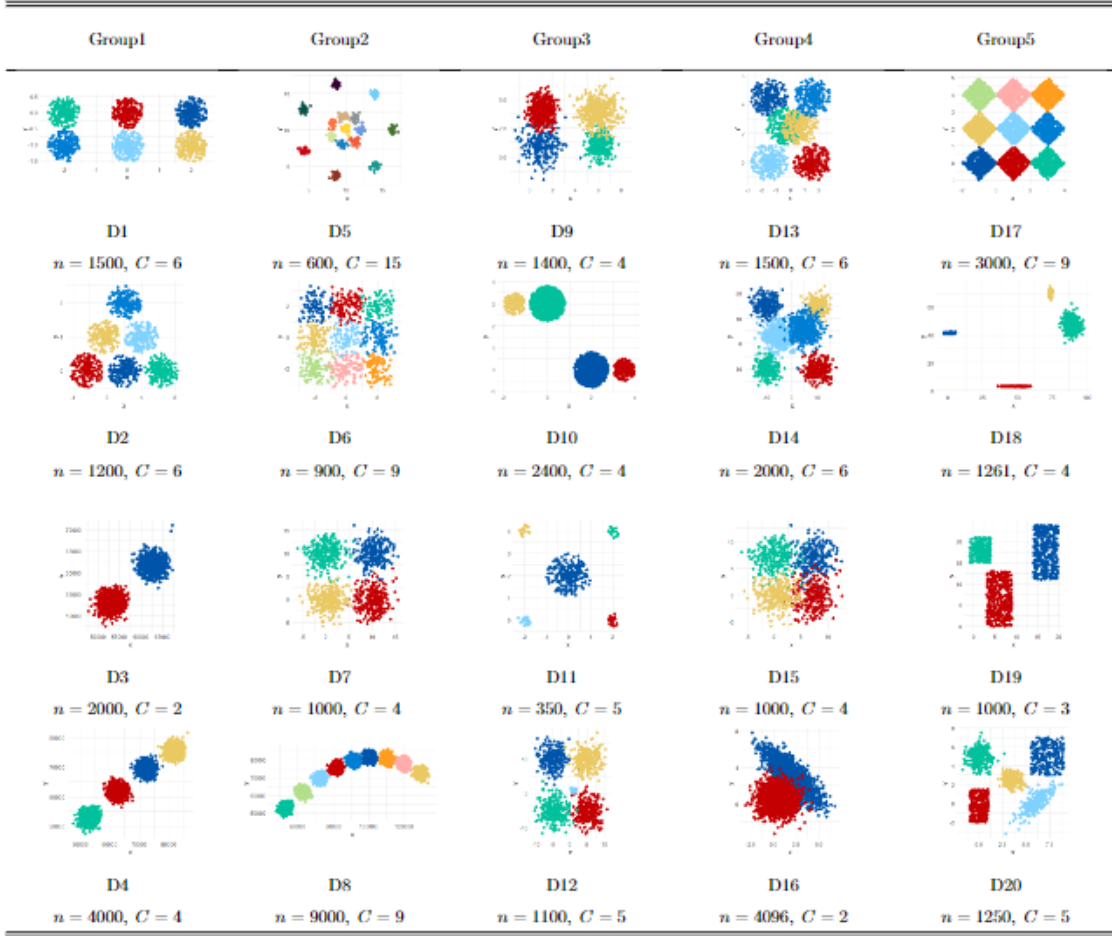
Group2: non-overlapped $D5 - D8$

Group3: different size or density $D9 - D12$

Group4: overlapped $D13 - D16$

Group5: non-round shape $D17 - D20$.

The datasets' plots and specifications are presented in Figure 2. Most datasets were generated from Gaussian distributions, with varying means and variances, except for D17–D20, which combine Gaussian and Uniform distributions.

Figure 2: Artificial datasets

Group1	Group2	Group3	Group4	Group5
D1	D5	D9	D13	D17
$n = 1500,\ C = 6$	$n = 600,\ C = 15$	$n = 1400,\ C = 4$	$n = 1500,\ C = 6$	$n = 3000,\ C = 9$
D2	D6	D10	D14	D18
$n = 1200,\ C = 6$	$n = 900,\ C = 9$	$n = 2400,\ C = 4$	$n = 2000,\ C = 6$	$n = 1261,\ C = 4$
D3	D7	D11	D15	D19
$n = 2000,\ C = 2$	$n = 1000,\ C = 4$	$n = 350,\ C = 5$	$n = 1000,\ C = 4$	$n = 1000,\ C = 3$
D4	D8	D12	D16	D20
$n = 4000,\ C = 4$	$n = 9000,\ C = 9$	$n = 1100,\ C = 5$	$n = 4096,\ C = 2$	$n = 1250,\ C = 5$

Note: n and C are the number of data points and the true number of clusters, respectively

To evaluate the efficiency of our proposed index in comparison to other well-known indices, we consider two criteria. Firstly, we compare the number of datasets for which each index accurately detects the known number of clusters. Secondly, we analyze the average rank to which the actual number of clusters corresponds. A well-performing index should yield an average rank close to 1.

Table 5 illustrates the outcomes of these comparisons for various values of m (1.5, 2, 4). Our proposed index demonstrates superior performance in terms of both the count of correctly detected datasets and the average rank across different m values. While PBM excels for small m, its performance diminishes as m increases. XB, Tang, and Kwon2 exhibit similar behaviors, aligning closely for $m = 1.5$ and $m = 2$, with Tang and Kwon2 slightly outperforming XB. Kwon2, as asserted in [18], emerges as the best performer among the three for $m = 4$. Kwon2 showcases compatibility with FCM for $m = 2$, yielding the second-best overall results.

Table 5: Artificial datasets

Datasets	C	XB 1.5	XB 2	XB 4	PBM 1.5	PBM 2	PBM 4	Tang 1.5	Tang 2	Tang 4	WL 1.5	WL 2	WL 4	GC 1.5	GC 2	GC 4	Kwon2 1.5	Kwon2 2	Kwon2 4	WP 1.5	WP 2	WP 4
D1	6	1	1	3	1	1	5	1	1	2	1	1	2	5	1	5	1	1	1	1	1	1
D2	6	1	1	2	1	1	5	1	1	1	2	2	4	1	1	5	1	1	1	1	1	1
D3	2	1	1	1	1	1	1	1	1	1	1	1	1	8	1	1	1	1	1	1	1	1
D4	4	1	1	2	1	1	3	1	1	2	2	1	2	7	1	3	1	1	1	1	1	1
D5	15	1	1	-	1	1	-	1	1	-	2	4	-	2	1	-	1	2	-	1	1	-
D6	9	1	1	2	2	8	8	1	1	2	7	5	5	6	8	8	1	1	1	1	1	1
D7	4	1	1	1	1	1	2	1	1	1	1	1	1	1	1	3	1	1	1	1	1	1
D8	9	8	7	8	1	2	8	6	6	8	8	9	10	6	1	8	6	3	3	1	1	1
D9	4	1	1	1	1	1	3	1	1	1	1	1	1	6	1	3	1	1	1	1	1	1
D10	4	2	2	2	1	1	2	2	2	2	1	2	2	6	1	3	3	1	2	1	1	4
D11	5	1	1	-	1	4	-	1	1	-	1	1	-	5	1	-	1	1	-	1	1	-
D12	5	2	2	3	1	2	4	2	2	3	2	2	2	6	2	4	2	2	2	1	1	1
D13	6	4	5	3	2	2	3	4	5	3	4	4	3	4	3	5	6	4	3	3	3	1
D14	6	2	2	2	1	1	5	2	2	2	1	1	2	4	1	5	1	1	2	1	1	1
D15	4	1	1	1	1	1	2	1	1	1	1	1	1	1	1	3	1	1	1	1	1	1
D16	2	9	8	2	2	1	1	9	8	2	3	7	1	9	1	1	9	9	9	2	2	2
D17	9	1	1	1	1	7	8	1	1	1	4	4	7	1	6	8	1	1	1	1	1	1
D18	4	1	2	3	1	1	3	1	2	2	1	6	4	7	3	3	1	1	2	1	1	1
D19	3	1	1	1	5	2	2	1	1	1	2	2	1	8	1	2	4	2	1	3	2	3
D20	5	1	2	2	1	1	3	1	2	2	2	1	2	6	1	4	1	1	2	1	1	1
# correct C		14	12	6	<u>16</u>	13	2	14	12	7	9	9	6	4	15	2	14	14	<u>10</u>	**17**	**17**	**15**
Average		2.05	2.10	2.22	<u>1.35</u>	2.00	3.78	1.95	2.05	2.06	2.35	2.80	2.83	4.95	1.85	4.11	2.2	<u>1.80</u>	<u>1.94</u>	**1.25**	**1.20**	**1.33**

Note: The best and second best results are bold and underlined, respectively.
This applies to all the results tables below.

When assessing each index's performance within specific dataset groups, it's evident that existing indexes excel in well-separated datasets. On the contrary, our proposed index performs effectively across all dataset groups, with slightly lower performance in Groups 4 and 5.

4.2.2 Real-world datasets

Table 6: Real world datasets speculations

Dataset	No. instances	No. features	No. classes
BCW	569	30	2
SEED	210	7	3
ION	351	33	2
Iris	150	4	2,3
Wine	178	13	3

Moving on to real-world datasets, we analyzed five datasets from the UCI repository [40]: Breast Cancer Wisconsin (BCW), Seed, Ionosphere (ION), Iris, and Wine. The specifications of these datasets are presented in Table 6. Notably, it's recognized that clustering the iris data can result in either 2 or 3 partitions, as indicated in [41].

Table 7: Real-world datasets

Data	K	XB			PBM			Tang			WL			GC			Kwon2			WP		
		1.5	2	4	1.5	2	4	1.5	2	4	1.5	2	4	1.5	2	4	1.5	2	4	1.5	2	4
BcW	2	1	1	1	1	1	1	1	1	1	1	1	1	1	1	1	1	1	1	1	1	1
SEED	3	2	2	2	1	2	2	2	2	2	2	2	2	1	2	2	2	2	1	4	4	1
ION	2	2	1	1	1	1	1	2	1	1	1	1	1	1	1	1	4	1	1	1	1	1
Iris	2,3	1	1	1	1	1	1	1	1	1	1	1	1	7	1	1	5	3	1	1	1	5
Wine	3	1	1	-	2	2	-	1	1	-	2	1	-	1	2	-	1	1	-	1	1	-
# correct C		3	4	3	4	3	3	3	4	3	3	4	3	4	3	3	2	3	4	4	4	3
Average		1.40	1.20	1.25	1.20	1.40	1.25	1.40	1.20	1.25	1.40	1.20	1.25	2.20	1.40	1.25	2.60	1.60	1.00	1.60	1.60	2.00

The experimental results are presented in Table 7. Our proposed index demonstrates the best performance in terms of correctly detected counts for $m = 1.5$ and $m = 2$ and performs moderately well for $m = 4$. XB, PBM, Tang, WL, and GC consistently perform well for all values of m. Kwon2 excels particularly for $m = 4$, as claimed. It's important to note that interpreting index performance based on real-world datasets can be challenging, as hidden subgroups might exist within labeled groups or labeled groups could be subsets of larger groups.

Remark 4.1 *We emphasize that the results of the WP index are based on the default γ value of $7m^2/4$. For the iris data with $m = 4$, our index can correctly detect the number of clusters if we reduce γ to 1. It's well-known that the two groups in the iris data are overlapped, and using a larger m is more reasonable. Thus, Proposition 3.6 implies that the default γ might be too large, as it reduces the fuzziness level during index computation. However, we report the results using the default γ as prior information about the dataset's characteristics is often not available. If users possess prior knowledge that the data is highly overlapped or very well separated, then choosing a larger or smaller γ accordingly can enhance the performance of our index.*

4.2.3 Simulated datasets with second option
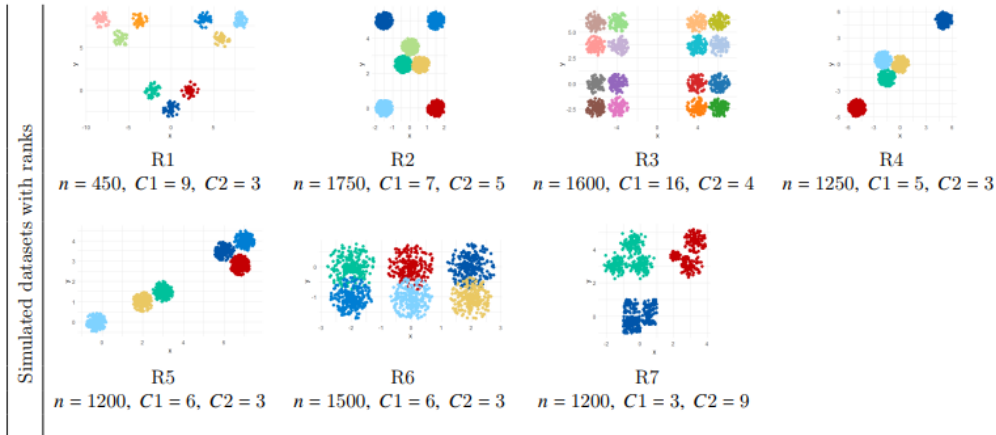
Note: n, $C1$, and $C2$ are the number of data points, the first and secondary options for the number of clusters, respectively.

Figure 3: Simulated datasets with second option

In this subsection, we assess the performance of each index on our simulated datasets that have multiple viable options for the number of clusters. The plots of all these datasets with the first two ranks of the optimal number of clusters are displayed in Fig. 3. We evaluate indexes based on their

capability to detect both optimal and sub-optimal numbers of clusters. Table 8 shows the number of clusters detected by each index. Since we are not aware of any works considering secondary options, we establish the R-score for comparing CVI performance as the sum of sc1 and sc2 defined below, which quantifies an index's success in detecting optimal and sub-optimal clusters. We give the first priority to the optimal number of clusters and fairly assign equal gaps between any two cases. The larger R-score indicates the better performance in detecting both options.

$$
sc1 = \begin{cases} 3 & \text{if the optimal number of cluster is at rank 1.} \\ 2 & \text{if the optimal number of cluster is at rank 2.} \\ 1 & \text{if the optimal number of cluster is at rank 3.} \end{cases}
$$

$$
sc2 = \begin{cases} 2 & \text{if the secondary number of cluster is at rank 2.} \\ 1 & \text{if the secondary number of cluster is at rank 1 or 3.} \end{cases}
$$

Table 8: Simulated datasets with second option

Datasets	C1	C2	XB			PBM			Tang			WL			GC			Kwon2			WP		
			1	2	3	1	2	3	1	2	3	1	2	3	1	2	3	1	2	3	1	2	3
R1	9	3	9	3	8	9	10	11	3	9	8	9	12	11	9	10	11	9	3	8	9	3	15
R2	7	5	5	4	7	7	6	8	5	7	6	5	10	9	7	8	6	5	7	6	7	5	6
R3	16	4	4	16	8	4	5	6	4	16	8	16	20	19	4	5	8	4	15	8	16	18	4
R4	5	3	3	5	2	5	3	4	3	5	2	3	5	8	5	6	7	5	3	10	5	3	8
R5	6	3	2	3	6	6	3	4	2	3	6	6	8	9	6	7	8	6	7	8	6	3	10
R6	6	3	9	4	8	4	6	5	9	4	8	8	7	6	6	5	4	9	8	7	2	4	6
R7	3	9	3	9	2	4	3	5	3	9	8	9	13	12	3	4	6	9	3	10	8	3	12
R-Score	35			21			21			20			15			21			20			27		

From Table 8, our proposed index demonstrates strong performance in this task. It correctly detects the first and second ranks for four out of seven datasets, while for the remaining three datasets, it places the optimal number of clusters within the first three ranks.

Moreover, according to the defined score criteria, WP achieves a score of 27, outperforming XB (21), PBM (21), Tang (20), WL (15), GC (21), and Kwon2 (24).

4.2.4 Image datasets

Figure 4: Image datasets

In this subsection, we analyze five RGB-colored images from BSDS 300 [42], as shown in Fig. 4. As each image is too large for GC and WP due to their complexity (see Table 1), we first reduce the image quality to 80×120 pixels before applying the indexes. The range of optimal numbers of clusters for each image is determined based on the clarity of the main object. For instance, in IMG1, the flower is clearly visible at $c = 2$, while $c = 3$ and $c = 4$ provide more detail in the pollen area. Similarly, $c \in [2, 4]$ is acceptable for IMG2 to capture the starfish, while higher values introduce noise. For the last three images, $c > 2$ increases unnecessary noise around the main objects, making $c = 2$ the most reasonable choice. As image analysis is inherently subjective, we state only ranges without explicit rankings. Again as we are not aware of any works considering secondary options in the context of image clustering, we self-establish the I-Score criterion as

$$
ISC = \begin{cases}
3 & \text{if } r_i \in A \text{ for all } i \\
2.5 & \text{if } r_i \in A \text{ for only } i = 1, 2 \\
2 & \text{if } r_i \in A \text{ for only } i = 1, 3 \\
1.5 & \text{if } r_i \in A \text{ for only } i = 1 \text{ or } i = 2, 3 \\
1 & \text{if } r_i \in A \text{ for only } i = 2 \\
0.5 & \text{if } r_i \in A \text{ for only } i = 3
\end{cases}
$$

19

where A represents the set of acceptable numbers of clusters, and r_i, $i = 1, 2, 3$, represent the first three ranks from an index, respectively. To be more precise, we rank the situations from best to worst in detecting hidden number of clusters within an image dataset. Then we fairly assign equal gaps between any two cases. Clearly, the larger I-score indicates the better performance on an image dataset.

Data	C	XB			PBM			Tang			WL			GC			Kwon2			WP		
		1	2	3	1	2	3	1	2	3	1	2	3	1	2	3	1	2	3	1	2	3
IMG1	[2,4]	5	4	2	4	8	3	5	4	3	5	8	3	5	3	4	5	4	10	4	2	8
IMG2	[2,4]	2	3	5	3	4	5	2	3	5	2	3	4	2	3	4	7	9	5	6	3	8
IMG3	2	2	3	6	3	4	5	2	3	6	2	3	6	2	3	5	6	2	5	2	8	3
IMG4	2	2	4	3	6	7	8	2	4	3	2	6	9	2	3	4	7	10	9	2	6	7
IMG5	2	2	3	7	2	3	4	2	3	7	2	3	4	2	6	7	2	10	9	2	4	10
I-Score	10.5	<u>8.5</u>			6			<u>8.5</u>			8			9			3.5			8		

Table 9: Image datasets

The results are shown in Table 9. Among the indexes, GC scores the highest with 9 out of 10.5 points. XB, Tang, WP, and WL also perform well, achieving scores of 8.5, 8.5, 8, and 8, respectively.

4.2.5   Analysis of the WP index

Based on our experiments on the four types of datasets, the WP index has the main advantages that its performance remains stable for more complicated datasets as in Table 5 and it provides the best result in detecting secondary options when the two options are not consecutive as shown in Table 8. However, as in Table 9, it detects mostly the first option when all the options are successive as in the image data case. The main disadvantage of our index is the computational time as discussed earlier and it requires some undersampling when handling large datasets including image datasets. This may result in a slightly worse performance.

5   Conclusion

In this study, we have introduced the WP index, inspired by the Wiroonsri index. Unlike the original index, our proposed WP index is potentially applicable to any soft clustering method that provides membership degrees. However, the performance has been tested only on the FCM algorithm. It is defined based on the correlation between the actual distance between a pair of data points and the distance between adjusted centroids considering the membership degrees. The primary motivations behind developing this new index and introducing it as an option among the existing fuzzy cluster validity indices are as follows:

1. **Unique concept and precision:** WP index operates under a distinctive concept compared to other existing indices, yet it exhibits a high degree of precision in detecting the optimal number of clusters.

2. **Sub-optimal detection:** WP index offers the advantage of identifying sub-optimal numbers of clusters, allowing users to make personalized selections.

3. **Flexible parameter:** WP index has a fuzziness parameter γ where users can select, though we recommend to use our default value.

We compare our proposed index with XB, PBM, Tang, WL, Generalized C, and Kwon2 indexes across four types of datasets: artificial datasets, real-world datasets, simulated datasets with second option, and image datasets. We use the FCM algorithm with fuzziness parameter values ranging from 1.5 to 4. For the first two types of datasets, we assess performance based on the number of correctly identified optimal clusters and the average rank across all datasets where the optimal cluster numbers are applicable. For the last two dataset types, we establish new scoring criteria based on the first three options provided by each index. Our evaluation approach and results are summarized as follows.

1. Among the 20 artificial datasets, the WP index clearly demonstrates superior performance in all aspects.

2. Across the five real-world datasets, the WP index stands out as one of the top performers when the fuzziness parameter m is set to 1.5 and 2, and it shows moderate performance for $m = 4$.

3. Among the seven simulated datasets with second option, the WP index outperforms the other indices based on our scoring criterion.

4. Across the five image datasets, the WP index achieves moderate performance according to the defined criterion.

We also conduct a sensitivity analysis of the WP index based on the fuzziness parameter γ. Our default parameter of $7m^2/4$ provides low sensitivity in most cases and has the best performance overall. Though a larger γ is slightly more suitable in the well-separated case, it maybe hard to know whether datasets are well-separated or not in reality. There maybe some other values of γ which are more appropriate in different and more complicated contexts, nevertheless, using our default value is recommended as datasets are usually blind especially in higher dimensional. Analyzing this parameter under different and more complicated contexts would be an interesting future research which will benefit users with some insights on their datasets.

The primary concern with the WP index is its reliance on computing distances between all pairs of data points, rendering it unsuitable for direct application to large datasets. It is important to note that due to this limitation, it is not compatible with big data scenarios. However, we put forward a potential solution for handling big data in the future: by initially undersampling a large dataset and then applying the WP index. While this approach has not been thoroughly tested yet, preliminary results suggest its effectiveness, particularly evident when we deliberately lower the image quality in our image data experiment. Enhancing the index's performance within this context and comparing it with other recent CVIs mentioned in the introduction present an unexplored avenue for future research.

References

[1] C. C. Aggarwal and C. K. Reddy, "Data clustering," *Algorithms and Applications*, p. 93, 2014.

[2] E. Min, X. Guo, Q. Liu, G. Zhang, J. Cui, and J. Long, "A survey of clustering with deep learning: From the perspective of network architecture," *IEEE Access*, vol. 6, pp. 39501–39514, 2018.

[3] Y. Xie, J. Tian, and X. X. Zhu, "Linking points with labels in 3d: A review of point cloud semantic segmentation," *IEEE Geoscience and Remote Sensing Magazine*, vol. 8, no. 4, pp. 38–59, 2020.

[4] Y. Guo, H. Wang, Q. Hu, H. Liu, L. Liu, and M. Bennamoun, "Deep learning for 3d point clouds: A survey," *IEEE Transactions on Pattern Analysis and Machine Intelligence*, vol. 43, no. 12, pp. 4338–4364, 2021.

[5] H. Chen, T. Xie, M. Liang, W. Liu, and P. X. Liu, "A local tangent plane distance-based approach to 3d point cloud segmentation via clustering," *Pattern Recognition*, vol. 137, p. 109307, 2023.

[6] M. Bicego, "Disrfc: a dissimilarity-based random forest clustering approach," *Pattern Recognition*, vol. 133, p. 109036, 2023.

[7] Pourbahrami, S. A neighborhood-based robust clustering algorithm using Apollonius function kernel. *Expert Systems With Applications*. **248** pp. 123407 (2024).

[8] D. Kumar and J. C. Bezdek, "Clustering tendency assessment for datasets having inter-cluster density variations," in *2020 International Conference on Signal Processing and Communications (SPCOM)*, pp. 1–5, 2020.

[9] J. C. Dunn, "A fuzzy relative of the isodata process and its use in detecting compact well-separated clusters," *Journal of Cybernetics*, vol. 3, no. 3, pp. 32–57, 1973.

[10] J. C. Bezdek, R. Ehrlich, and W. Full, "Fcm: The fuzzy c-means clustering algorithm," *Computers & Geosciences*, vol. 10, no. 2, pp. 191–203, 1984.

[11] D. T. Anderson, J. C. Bezdek, M. Popescu, and J. M. Keller, "Comparing fuzzy, probabilistic, and possibilistic partitions," *IEEE Transactions on Fuzzy Systems*, vol. 18, no. 5, pp. 906–918, 2010.

[12] X. Xie and G. Beni, "A validity measure for fuzzy clustering," *IEEE Transactions on Pattern Analysis and Machine Intelligence*, vol. 13, no. 8, pp. 841–847, 1991.

[13] Y. Fukuyama, "A new method of choosing the number of clusters for fuzzy c-means method," in *Proc. 5th Fuzzy System Symp.*, pp. 247–250, 1989.

[14] M. K. Pakhira, S. Bandyopadhyay, and U. Maulik, "Validity index for crisp and fuzzy clusters," *Pattern recognition*, vol. 37, no. 3, pp. 487–501, 2004.

[15] Y. Tang, F. Sun, and Z. Sun, "Improved validation index for fuzzy clustering," in *Proceedings of the 2005, American Control Conference, 2005.*, pp. 1120–1125 vol. 2, 2005.

[16] C. H. Wu, C. S. Ouyang, L. W. Chen, and L. W. Lu, "A new fuzzy clustering validity index with a median factor for centroid-based clustering," *IEEE Transactions on Fuzzy Systems*, vol. 23, no. 3, pp. 701–718, 2015.

[17] S. H. Kwon, "Cluster validity index for fuzzy clustering," *Electronics letters*, vol. 34, no. 22, pp. 2176–2177, 1998.

[18] S. H. Kwon, J. Kim, and S. H. Son, "Improved cluster validity index for fuzzy clustering," *Electronics Letters*, vol. 57, no. 21, pp. 792–794, 2021.

[19] H. Mittal and M. Saraswat, "A new fuzzy cluster validity index for hyperellipsoid or hyperspherical shape close clusters with distant centroids," *IEEE Transactions on Fuzzy Systems*, vol. 29, no. 11, pp. 3249–3258, 2021.

[20] J. C. Bezdek, M. Moshtaghi, T. Runkler, and C. Leckie, "The generalized c index for internal fuzzy cluster validity," *IEEE Transactions on Fuzzy Systems*, vol. 24, no. 6, pp. 1500–1512, 2016.

[21] L. J. Hubert and J. R. Levin, "A general statistical framework for assessing categorical clustering in free recall.," *Psychological bulletin*, vol. 83, no. 6, p. 1072, 1976.

[22] M. Popescu, J. C. Bezdek, T. C. Havens, and J. M. Keller, "A cluster validity framework based on induced partition dissimilarity," *IEEE Transactions on Cybernetics*, vol. 43, no. 1, pp. 308–320, 2013.

[23] Liu, F., Wang, J. & Liu, Y. IMI2: A fuzzy clustering validity index for multiple imbalanced clusters. *Expert Systems With Applications*. **238** pp. 122231 (2024).

[24] N. Wiroonsri, "Clustering performance analysis using a new correlation-based cluster validity index," *Pattern Recognition*, p. 109910, 2024.

[25] Q. Li, S. Yue, Y. Wang, M. Ding, and J. Li, "A new cluster validity index based on the adjustment of within-cluster distance," *IEEE Access*, vol. 8, pp. 202872–202885, 2020.

[26] M. Naderipour, M. H. Fazel Zarandi, and S. Bastani, "A fuzzy cluster-validity index based on the topology structure and node attribute in complex networks," *Expert Systems with Applications*, vol. 187, p. 115913, 2022.

[27] H. Y. Wang, J. S. Wang, and G. Wang, "Combination evaluation method of fuzzy c-mean clustering validity based on hybrid weighted strategy," *IEEE Access*, vol. 9, pp. 27239–27261, 2021.

[28] S. D. Nguyen, V. S. T. Nguyen, and N. T. Pham, "Determination of the optimal number of clusters: A fuzzy-set based method," *IEEE Transactions on Fuzzy Systems*, vol. 30, no. 9, pp. 3514–3526, 2022.

[29] H. Mittal and M. Saraswat, "A new fuzzy cluster validity index for hyperellipsoid or hyperspherical shape close clusters with distant centroids," *IEEE Transactions on Fuzzy Systems*, vol. 29, no. 11, pp. 3249–3258, 2021.

[30] M. Niemelä, S. Äyrämö, and T. Kärkkäinen, "Toolbox for distance estimation and cluster validation on data with missing values," *IEEE Access*, vol. 10, pp. 352–367, 2022.

[31] B. Tavakkol, J. Choi, M. K. Jeong, and S. L. Albin, "Object-based cluster validation with densities," *Pattern Recognition*, vol. 121, p. 108223, 2022.

[32] L. E. Brito da Silva, N. Rayapati, and D. C. Wunsch, "Incremental cluster validity index-guided online learning for performance and robustness to presentation order," *IEEE Transactions on Neural Networks and Learning Systems*, vol. 34, no. 10, pp. 6686–6700, 2023.

[33] N. Wiroonsri and O. Preedasawakul, *UniversalCVI: Hard and Soft Cluster Validity Indices*, 2023. R package version 1.1.0.

[34] RStudio Team, *RStudio: Integrated Development Environment for R*. RStudio, PBC., Boston, MA, 2020.

[35] D. Meyer, E. Dimitriadou, K. Hornik, A. Weingessel, and F. Leisch, *e1071: Misc Functions of the Department of Statistics, Probability Theory Group (Formerly: E1071), TU Wien*, 2022. R package version 1.7-12.

[36] K. L. Wu, "Analysis of parameter selections for fuzzy c-means," *Pattern Recognition*, vol. 45, no. 1, pp. 407–415, 2012.

[37] P. Fränti and S. Sieranoja, "K-means properties on six clustering benchmark datasets," 2018.

[38] O. Preedasawakul and N. Wiroonsri, "FuzzyDatasets: Benchmarks datasets for clustering." `https://github.com/O-PREEDASAWAKUL/FuzzyDatasets`, 2023.

[39] T. Barton, "Clustering benchmarks," 2019.

[40] M. Lichman, "Uci machine learning repository," 2013.

[41] D. W. Kim, K. H. Lee, and D. Lee, "On cluster validity index for estimation of the optimal number of fuzzy clusters," *Pattern Recognition*, vol. 37, no. 10, pp. 2009–2025, 2004.

[42] D. Martin, C. Fowlkes, D. Tal, and J. Malik, "A database of human segmented natural images and its application to evaluating segmentation algorithms and measuring ecological statistics," in *Proc. 8th Int'l Conf. Computer Vision*, vol. 2, pp. 416–423, July 2001.